J. Phys. A: Math. Gen. 25 (1992) 6283–6296. Printed in the UK

Clustered motion in symplectic coupled map systems

Tetsuro Konishi†§ and Kunihiko Kaneko‡||

† Department of Physics, School of Science, Nagoya University, Nagoya, 464-01, Japan
‡ Department of Pure and Applied Sciences, College of Arts and Sciences, University of Tokyo, Komaba, Meguro-ku, Tokyo, 153, Japan

Received 20 November 1991, in final form 7 May 1992

Abstract. Clustered motion of particles is found in Hamiltonian dynamics of symplectic coupled map systems. Particles assemble and move with strong correlation. The motion is chaotic but is distinguishable from random chaotic motion. Lyapunov analysis distinguishes global instability from local fluctuations. Clustered motions have finite lifetime. They have fractal geometric structure in the phase space, as the orbits are trapped to ruins of KAM tori and islands.

1. Introduction

Order and chaos are often considered to be opposite notions in nature. One may associate order with stable and regular behaviour, and chaos with unstable and random behaviour. In this paper we discuss a new kind of cluster-like order in Hamiltonian systems which is at the same time chaotic.

Ordering processes are typically found in dissipative systems, where, after sufficiently long time, the dynamics leads to an ordered state represented by an attractor. Most studies on pattern formation belong to this class of transient process towards ordered attractors. For such systems ordering is a rather trivial evolution, since the dynamics is such that the system evolves in the direction of increasing order. On the other hand, order formation in Hamiltonian systems is non-trivial, because long-time behaviour of Hamiltonian systems is considered to be well described by thermal equilibrium.

Hamiltonian systems and their chaotic dynamics have been intensively studied [1, 2]. The phase space of typical Hamiltonian systems is known to have both regular and irregular orbits. Regular orbits consist of KAM tori and islands, which correspond to quasi-periodic motion, whereas irregular ones represent chaotic orbits. For Hamiltonian systems with many degrees of freedom, local instability often leads the system to uniformly random states, i.e. thermal equilibrium.

Uniform thermalization, however, is not the *only* feature of chaotic motion in Hamiltonian systems. Order formation must be an emergent property in a Hamiltonian system, as is seen in astrophysics (globular stellar clusters), microclusters [3], and in many other fields. Even pattern formation in dissipative systems should be initially described by a Hamiltonian system, if we start from a molecular level description.

§ E-mail address: c42636a@nucc.cc.nagoya-u.ac.jp
|| E-mail address: chaos@tansei.cc.u-tokyo.ac.jp

0305-4470/92/236283+14$07.50

This paper is organized as follows. In the next section, a symplectic map model is introduced for the ordering in Hamiltonian system. The discovery of clustered motion is reported in section 3, with its qualitative aspects. Lyapunov spectra and vectors of the model are examined in section 4 and confirm that our model has two kinds of chaotic sea and that the global instability of the clustered motion is distinguished from local fluctuation of particles. In section 5 we study the origin of stability of the clustered motion by examining their lifetimes, phase space structure, and fluctuation properties. The clustered motion is then found to be sticky to ruins of KAM tori and islands. The last section is devoted to summary and discussion.

2. Model

In this paper we introduce a very simple model giving rise to order formation within Hamiltonian dynamics. We use a symplectic version of a coupled map lattice. Coupled map lattices are models defined on discrete space and time, so that they are particularly suitable for numerical investigation of phenomena in which long time behaviour is important [4–12].

We have N particles in our model (see figure 1). Each particle is on a unit circle, and the state of each particle is defined by its phase (position) $2\pi x_i$ and its conjugate momentum p_i. Temporal evolution is defined by

$$\begin{aligned} &(x_i, p_i) \mapsto (x_i', p_i') \qquad i = 1, 2, \ldots, N \\ &p_i' = p_i + \frac{K}{2\pi\sqrt{N-1}} \sum_{j=1}^{N} \sin 2\pi(x_j - x_i) \qquad K > 0 \\ &x_i' = x_i + p_i'. \end{aligned} \tag{1}$$

Since $K > 0$, the interaction term $(K/2\pi\sqrt{N-1}) \sin 2\pi(x_j - x_i)$ between two particles i and j is *attractive*.

This model includes the interaction between every pair of elements as in a gas, in contrast with the lattice type modelling. In a lattice model with a short-range interaction, a tendency to thermalization with uniform ergodic behaviour is observed [4, 10]. Although our model has a long-ranged gas-type interaction, our observation of a clustered state is also seen in a short-ranged gas-type interaction [13].

The model (1) satisfies the symplectic condition

$$\sum_{i=1}^{N} \mathrm{d}x_i \wedge \mathrm{d}p_i = \sum_{i=1}^{N} \mathrm{d}x_i' \wedge \mathrm{d}p_i' \tag{2}$$

so that the model can be regarded as a Poincaré map for a Hamiltonian system with $N + 1$ degrees of freedom. Another interpretation of our model is as a 'kicked' Hamiltonian, as in the standard mapping [1].

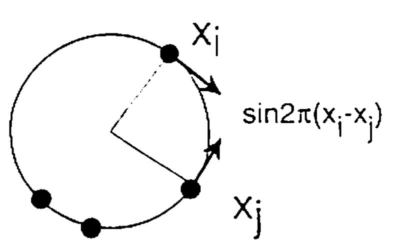

Figure 1. Our model. A two-particle interaction is schematically shown.

The total momentum is a constant of motion of the model (1)

$$\sum_{j=1}^{N} p_j = \text{constant} \tag{3}$$

so that the N degrees of freedom are decomposed into $1 \oplus (N-1)$, where '1' stands for the linear motion of the centre of mass. For $N = 2$, our model is reduced to the standard map of Chirikov and Taylor. The coupling constant K is scaled by $\sqrt{N-1}$ so that the model is expected to show extensive behaviour in the strongly chaotic regime $K \gtrsim 1$. In this regime correlation among particles is negligible and the force terms $(2\pi\sqrt{N-1})^{-1} K \sum_{j=1}^{N} \sin\left[2\pi(x_j(t) - x_i(t))\right]$ can be approximated by stochastic variables independent of the system size N. This approximation leads to proportionality of the diffusion coefficient to K^2, which is numerically confirmed for $K \gtrsim 1$ [4].

In this paper, we study a case with $K < 1$ where the motion of the particles forms a cluster.

3. Clustered state of particles

Figure 2 shows a typical example of clustered motion in the model (1). Particles initially distributed over a unit circle (with almost zero momenta) gradually move together to form a macro cluster. Some particles may not participate in cluster formation and wander around the cluster. These particles increase the entropy of the spatial configuration and serve to stabilize the clustered state. They play a role of effective dissipation for the dynamics of clustered motion, just like the 'halo' structure of globular stellar clusters. Roughly speaking, particles in a cluster show mutually oscillatory behaviour as is seen in chaos near elliptic (fixed) points. In our example the number of particles in the cluster is rather large (typically $N-2$ to N).

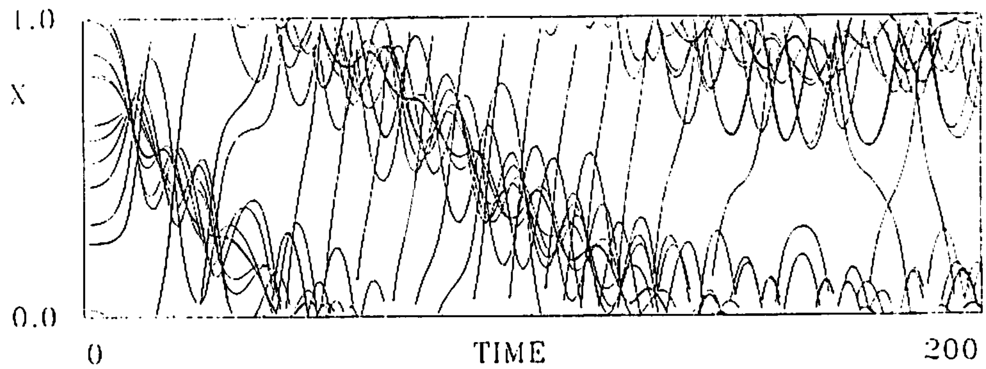

Figure 2. A typical example of clustered motion of the model (1). System size $N = 12$, and $K = 0.1$. Initial condition is chosen to be x_i = random, homogeneously distributed over $[0, 1)$, and $p_i = 0$.

'Absorption' or 'evaporation' of a particle to/from a cluster is also possible. In a weak nonlinear regime with a small number of particles, we have often observed temporal switches between N-particle-cluster and $(N-1)$-particle-cluster states through absorption and evaporation. Exchange of particles between a cluster and wandering states can occur, although the fluctuation in the number of particles in a cluster is very small.

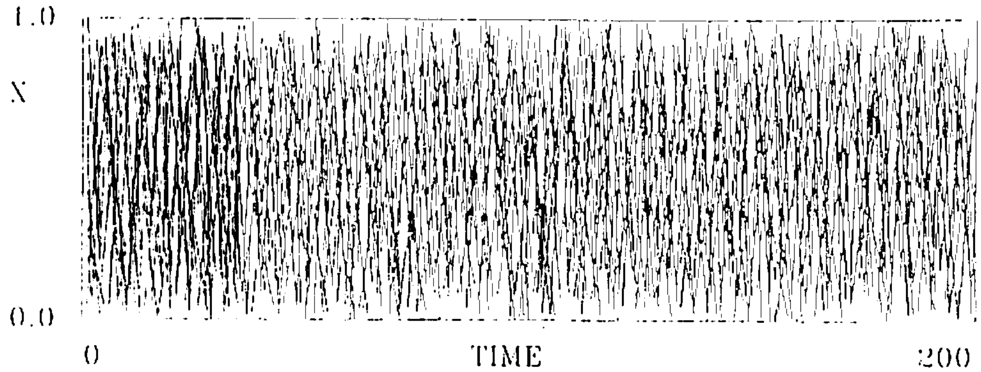

Figure 3. Random motion of the model (1). All parameters are the same as figure 2, except that initial condition is p_i = random homogeneously distributed over $[-0.5, 0.5)$.

The degree of clustering is evaluated by calculating the following quantity

$$Z \stackrel{\text{def}}{=} \left| \frac{1}{\sqrt{N}} \sum_{j=1}^{N} \exp\left(2\pi \mathrm{i} x_j\right) \right|^2 \tag{4}$$

$$= \begin{cases} N & \text{if all } x_j\text{'s are the same (fully clustered)} \\ 0 & \text{if } x_j\text{'s are uniformly distributed.} \end{cases} \tag{5}$$

A useful relation for Z is

$$\int_{[0,1)^N} \mathrm{d}^N x \, Z \delta\left(\sum_{j=1}^{N} x_j \right) = 1 \tag{6}$$

which means that the value of Z is unity for uncorrelated random motions (see figure 3). The δ function comes from the conservation of total momentum (3). The relation (6) serves as a criterion for clustering as

$$\text{a state is called 'clustered'} \stackrel{\text{def}}{=} Z > 1. \tag{7}$$

4. Lyapunov analysis

The clustered motion in figure 2 appears to be rather regular. It is, however, chaotic, as we can see from the Lyapunov spectra.

The Lyapunov spectrum is a characteristic of asymptotic orbital instability of dynamical systems. It is a set of real numbers with $2N$ elements $\{\lambda_1, \ldots, \lambda_{2N}\}$ defined by the eigenvalue spectrum of the squared Jacobi matrix

$$J(t) \stackrel{\text{def}}{=} \frac{\partial(p(t), x(t))}{\partial(p(0), x(0))} \tag{8}$$

$$\{\mathrm{e}^{2\lambda_1 T}, \ldots, \mathrm{e}^{2\lambda_{2N} T}\} = \text{eigenvalue spectrum of } {}^t J(T) J(T) \text{ as } T \to \infty. \tag{9}$$

For actual computation of exponents we use the standard method with Gram–Schmidt orthonormalization [14–15]. Other numerical methods to obtain Lyapunov spectrum are shown in [16]. If we arrange the exponents in the decreasing order

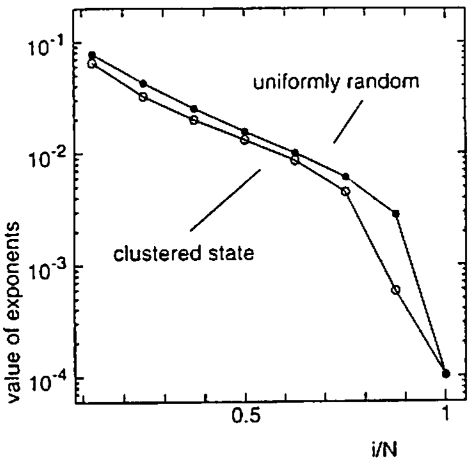

Figure 4. Lyapunov spectra for the model (1). $N = 16$, $K = 0.1$, sample = 100. The two spectra have different initial conditions. They are x_i = random, $|p_i| \ll 1$, and x_i = random, p_i = random for the 'clustered' state and the 'uniformly random' state, respectively.

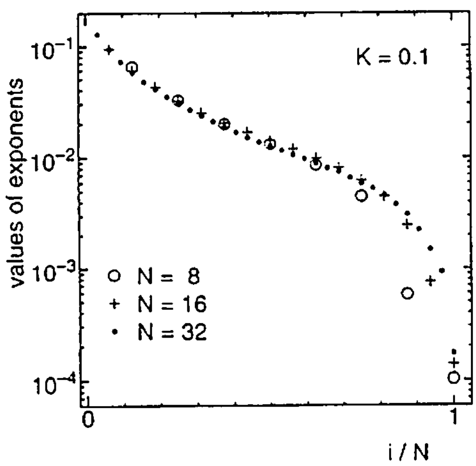

Figure 5. System size dependence of Lyapunov spectra for the clustered state. $K = 0.1$, $N = 8, 16, 32$.

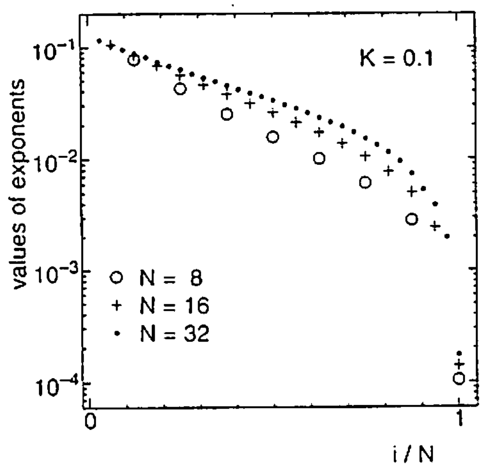

Figure 6. System size dependence of Lyapunov spectra for the uniformly random state. $K = 0.1$, $N = 8, 16, 32$.

$\lambda_1 \geqslant \lambda_2 \geqslant \cdots \geqslant \lambda_{2N}$, then we have $\lambda_i + \lambda_{2N+1-i} = 0$ from the symplectic condition (2), so that only the larger part of the whole spectrum is plotted.

Figure 4 shows Lyapunov spectra of the model (1). Even for clustered states we have positive Lyapunov exponents, which indicates that the clustered states are chaotic. For clustered states, the rescaled spectrum

$$\{\Lambda^{(N)}(q), 0 \leqslant q \leqslant 2 | \Lambda^{(N)}(i/N) \stackrel{\mathrm{def}}{=} \lambda_i \text{ as } N \to \infty\} \tag{10}$$

is almost invariant with a change in the system size N (see figure 5) [17–20].

For the uniformly random state, however, the spectrum varies with increasing N (figure 6). This result is rather puzzling, because the scaling of the coupling constant $K/2\pi\sqrt{N-1}$ is determined so that the behaviour of the model will be similar for all N if correlations between the particles are quite small. This may indicate the existence of a hidden correlation among particles in the (apparently) random state. The exponential behaviour of exponents $\lambda_j \propto \exp(-cj)$ in figure 6 is interesting, although its origin is not yet understood.

Note that there is only one exponent whose value is 0, which corresponds to the conservation of the total momentum (3). All the other exponents for a clustered state are positive, so that both the cluster itself and particles inside it move chaotically in time. Also, we can see a clear distinction between the spectra of a clustered state and a non-clustered (random) state, particularly for the exponent λ_{N-1}. This implies that two distinct chaotic regions coexist in phase space. (See section 5 for the coexistence of chaotic seas, which is shown in a two dimensional section of the phase space in figure 11.)

The existence of the almost zero exponent λ_{N-1} in the clustered state brings us to a viewpoint based on the following 'heat-bath picture'.

Suppose we have a cluster composed of $N-\ell$ particles. As long as most of the particles are in the cluster (i.e. $N \gg \ell$), it is natural to approximate the whole N-particle state by a composition of $(N-\ell)$-particle dynamics and the other ℓ particles acting as a heat bath for the cluster. Then the motion of $(N-\ell)$-particle dynamics is approximated by the coupled-map system of $(N-\ell)$ particles with noise, and we expect another null exponent for the $(N-\ell)$-particle dynamics. In this approximation, the heat bath can be regarded as behaving independently of the cluster as long as we neglect its interaction with the cluster. Hence the temporal average momentum of the heat bath is approximated by zero, which leads to another zero Lyapunov exponent. As is observed in figure 2, for example, a 'heat-bath' particle (a particle which does not belong to the cluster) moves almost freely over some period.

Although the heat bath picture is a zeroth approximation and the interaction between the cluster and the other particles must increase the value of the exponent, the existence of a small exponent in addition to the null one is consistent with the above picture. For the other exponents, their values are lowered slightly since the chaotic instability is lowered due to the decrease in the number of degrees of freedom involved.

This 'heat-bath' picture can be confirmed by the observation of Lyapunov vectors of the model. An analysis of Lyapunov vectors for lattice models is given in [21]. Lyapunov vectors are the principal axes of the ellipse evolving in the tangent space (see figure 7). If we follow the Lyapunov vector in accordance with the temporal evolution, we will see the directions *in* which instabilities arise. Hence if we obtain Lyapunov vectors for the *time-reversed* system, Lyapunov vectors represent the directions *from* which instabilities arise.

Examining each vector, we can judge whether the instability associated with an exponent arises from the clustered motion (macroscopic motion) or from internal thermal noise. Since each $2N$-dimensional Lyapunov vector consists of N pieces of 2-dimensional vectors, it represents infinitesimal displacements of each particle

$$(\mathrm{d}x^{(k)}, \mathrm{d}p^{(k)})\ (\in \mathrm{R}^{2N}) \ \Rightarrow \{v_i^{(k)} \stackrel{\mathrm{def}}{=} (\mathrm{d}x_i^{(k)}, \mathrm{d}p_i^{(k)}) \in \mathrm{R}^2, i = 1, 2, \ldots, N\} \tag{11}$$

where the index k denotes the vector corresponding to the kth exponent λ_k.

If the vectors $\{v_i^{(k)}, i = 1, 2, \ldots, N\}$ are well aligned, the corresponding Lyapunov vector is related to an instability of the collective motion of the cluster (see figure 8). If, on the other hand, the directions of vectors (11) are scattered, the corresponding instability comes from the uncorrelated motion of each particle and is regarded as thermal noise.

The degree of alignment of each vector (11) corresponding to λ_k can be measured by the following quantity

$$\begin{aligned}\sum_{i\neq j} |v_i^{(k)} - v_j^{(k)}|^2 &= \sum_{i\neq j} \left(|v_i^{(k)}|^2 + |v_j^{(k)}|^2 - 2\, v_i^{(k)} \cdot v_j^{(k)}\right) \\ &= 2(N-1) - 4 \sum_{i<j} v_i^{(k)} \cdot v_j^{(k)} \equiv 2(N-1) - 4\, s^{(k)}\end{aligned} \tag{12}$$

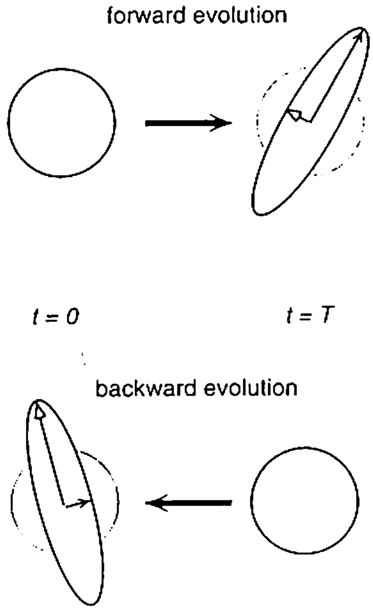

Figure 7. Lyapunov vectors for forward and backward time evolution. Initial infinitesimal spheres are shown to grow into ellipses. The black arrows represent the vectors that correspond to the largest Lyapunov exponent, and the white ones to the smallest Lyapunov exponent. Namely, length of the black arrow $\propto \exp(\lambda_{\max})$, and length of the white arrow $\propto \exp(\lambda_{\min})$ for forward evolution, and length of the black arrow $\propto \exp(-\lambda_{\max})$, and length of the white arrow $\propto \exp(-\lambda_{\min})$ for backward evolution. Remember that $\lambda_{\max} = -\lambda_{\min}$ as our model is symplectic.

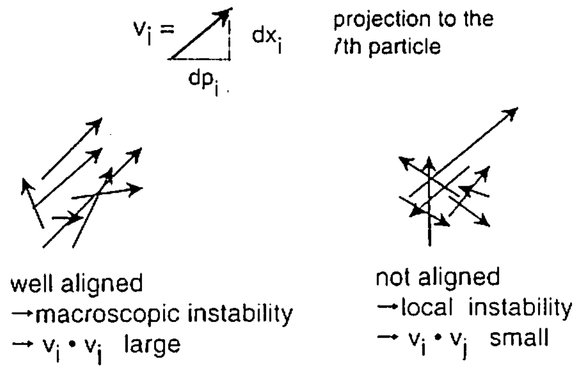

Figure 8. A Lyapunov vector is projected onto each particle. The difference between macroscopic and local instabilities are shown schematically.

where we adopt the following normalization of a Lyapunov vector

$$\sum_{i=1}^{N}\left[\left(\mathrm{d}x_i^{(k)}\right)^2+\left(\mathrm{d}p_i^{(k)}\right)^2\right] \equiv \sum_{i=1}^{N}|v_i^{(k)}|^2 = 1 \tag{13}$$

and the inner product of vectors for the kth exponent is defined by

$$s^{(k)} \stackrel{\mathrm{def}}{=} \sum_{i<j} v_i^{(k)} \cdot v_j^{(k)}. \tag{14}$$

Figure 9 shows each Lyapunov vector associated with two exponents; λ_1 the largest one, and λ_{N-1}. As is seen in the figure, the Lyapunov vector for λ_{N-1} looks quite well aligned. Thus the instability which corresponds to the exponent λ_{N-1} comes from the instability of the motion of the cluster. This is why the Lyapunov spectra (figure 4) of the clustered state and the random state differ for this exponent. This difference is quantitatively illustrated in table 1, where the values of the inner product of vectors $s^{(k)}$ are shown for the Lyapunov vectors corresponding to the exponents $\lambda_1, \lambda_2, \ldots, \lambda_k, \ldots, \lambda_{N-1}, \lambda_N$. Since the matrix ${}^tJ(T)J(T)$ is symmetric, the $2N \times 2N$-matrix $\{v_i^{(k)}\}$, $i = 1, 2, \ldots, N$, $k = 1, 2, \ldots, 2N$ is orthogonal and a sum rule $\sum_{k=1}^{N} s^{(k)} = 0$ holds.

Values of $s^{(k)}$ are bounded as

$$-\tfrac{1}{2}\ \ \text{(fully random direction)} \leqslant s^{(k)} \leqslant \tfrac{1}{2}(N-1)\ \ \text{(fully aligned)}. \tag{15}$$

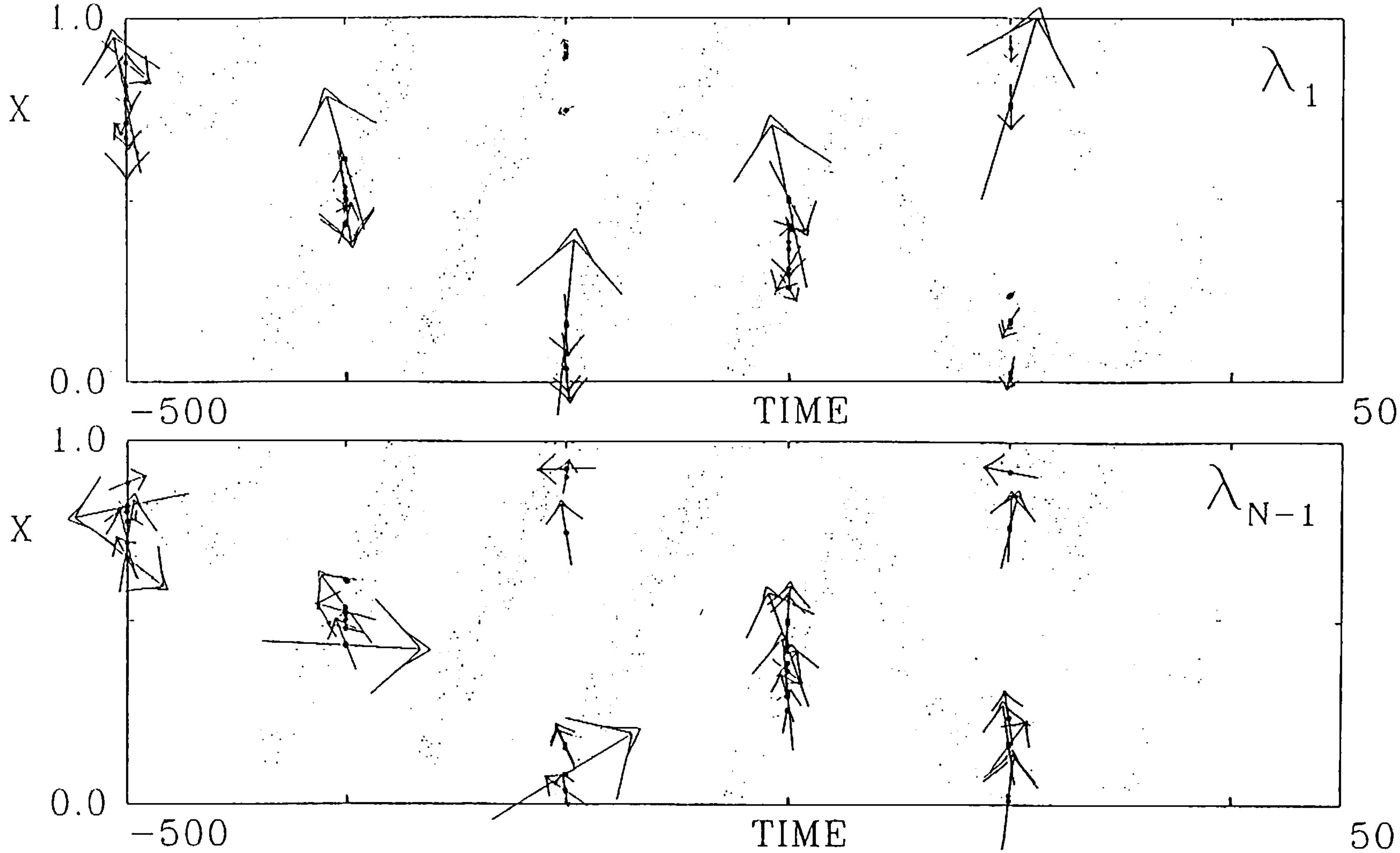

Figure 9. Temporal evolution of Lyapunov vectors for the exponents λ_1 and λ_{N-1}. Each Lyapunov vector (which is $2N$-dimensional) is decomposed as N pieces of two-dimensional vectors $(\mathrm{d}x_i, \mathrm{d}p_i)$, where i is the index of particles $(i = 1, 2, \ldots, N)$. Using the notation of figure 7, the infinitesimal sphere is set at $t = 0$ and it evolves backwards to $t = -500$. The dots scattered in the background represent positions of the particles which are in a clustered state.

Up to the $(N-2)$th vector, the inner product is close to $-1/2$, consistent with the random motion. For the $(N-1)$th vector the degree of alignment clearly differs between the random and clustered motions. For the random one, it is still close to $-1/2$, while the inner product is almost 0 for the clustered motion, implying the existence of some tendency for alignment. (The Nth vector is almost completely aligned since it represents a uniform translation corresponding to the conservation law of total momentum (3).)

Table 1. Values of the inner product $s^{(k)}$ (equation (14) for $N = 8$, see text).

k	$s^{(k)}$ (uniform)	$s^{(k)}$ (cluster)
1	−0.499	−0.499
2	−0.498	−0.498
3	−0.499	−0.498
4	−0.491	−0.489
5	−0.483	−0.497
6	−0.455	−0.470
7	−0.451	−0.078
8	3.378	3.033

5. Lifetime of clusters and phase space structure

Now we discuss the lifetime of clustered states. Since all parts of the chaotic sea in phase space are topologically and dynamically connected [22, 23] in a Hamiltonian system with many degrees of freedom, the chaos in the clustered state and the uniformly random chaos must be connected through a (thin) path. Thus the clustered states must have *finite* lifetime. Through time evolution, a clustered state switches to another chaotic state, random chaos. Of course, the reverse process is also possible. In the course of time evolution, the two types of motion are distinguished as quasistationary and metastable states, which makes possible the previous quantitative distinction between the two states.

Crossover from clustered to random chaos reminds us of the 'induction phenomenon' [24]. It is a transition from regular oscillation to chaotic motion found in weakly non-integrable systems. Nekhoroshev's theorem [25–28] can be applied to estimate the length of the period for the duration of a regular oscillation [29]. This estimate is possible because the induction phenomenon is a transition from a state

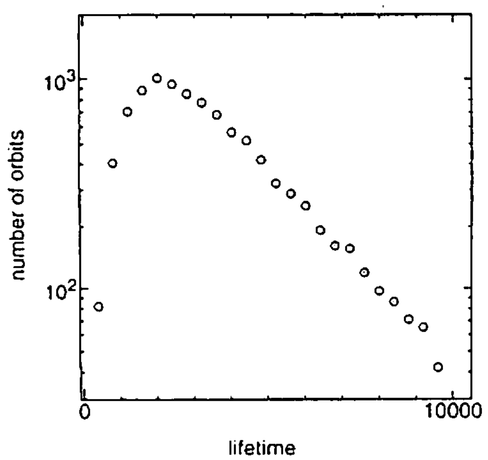

Figure 10. The lifetime distribution of clustered states. Initial condition: x_i = random, $p_i = 0$. System size $N = 8$, $K = 0.25$, total number of orbits = 10^3.

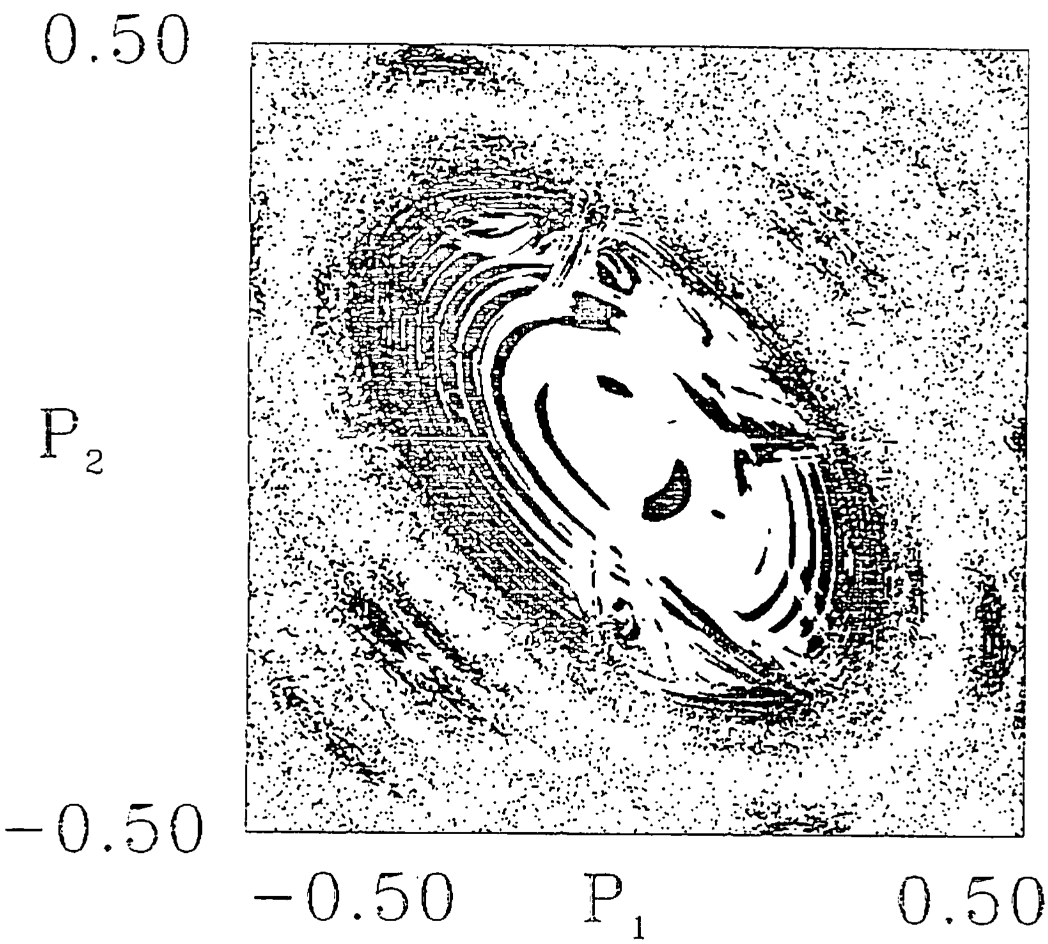

Figure 11. A 2D slice (p_1, p_2) of phase space. $N = 4$, $K = 0.3$. In the $(4 \times 2 =)$ 8-dimensional phase space, the slice is taken by setting the following six constraints; $x_1 = -0.075$, $x_2 = -0.025$, $x_3 = 0.025$, $p_3 = 0$, $\sum_1^4 x_i = \sum_1^4 p_i = 0$. The last two constraints come from conservation of the total momentum (3) so that the points shown in the figure have the same value of total momentum. We set 512×512 lattice points on the 2-dimensional section, take the points as initial conditions for time evolution. Among the initial conditions, dots are plotted for the initial points such that the temporal decay rate of the finite time maximal Lyapunov exponents $\lambda_{\max}(t)$ measured for $t = 200$ steps is faster than $1/\sqrt{t}$ are shown. The function $1/\sqrt{t}$ is adopted for convenience to distinguish between $\lambda_{\max}(t) =$ constant (chaos) and $\lambda_{\max}(t) \propto 1/t$ (tori, islands).

in the vicinity of a torus to chaos. Our transition from clustered to random states is clearly different from induction phenomena, since it is a switching between two types of chaos. For such types of crossover, we have as yet no theoretical method to estimate the lifetime of each state. The lifetime of clustered states also increases rather rapidly with the decrease of nonlinearity. This dependence suggests a possible estimate for the lifetime similar to Nekhoroshev's.

Figure 10 shows the distribution of the lifetime of clustered states for an 8-particle system. The initial condition is chosen to be $x_i =$ random, $p_i = 0$. This initial condition is chosen because clustered states appear to have large measure around the origin $(x, p) = 0$. For each orbit, the lifetime is defined as

$$\text{lifetime of clustered state} \stackrel{\text{def}}{=} \text{steps for which the value of } Z > 1 \tag{16}$$

where the quantity Z is defined in equation (6). The distributions for $K = 0.25, 0.3, 0.4, 0.5$ have an exponential tail.

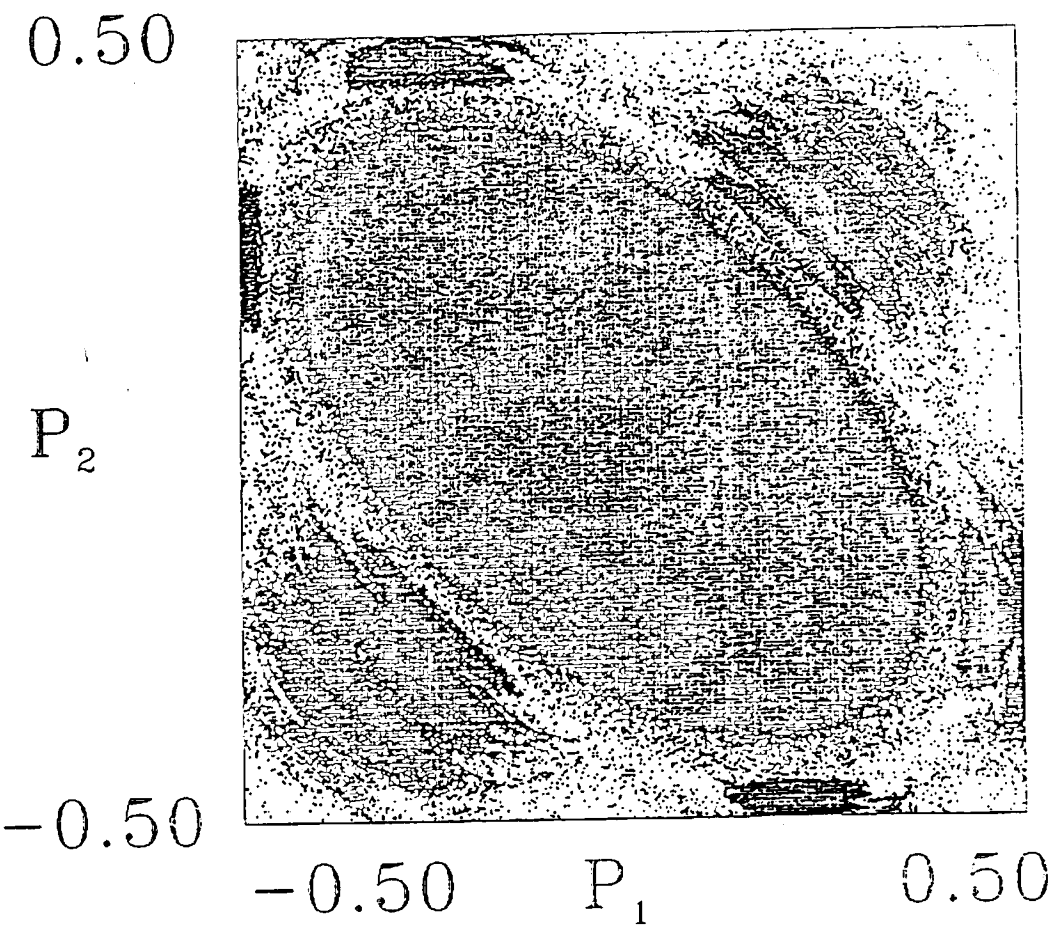

Figure 12. Same slice in the phase space as in figure 11. Among 512 x 512 initial conditions, points at which $Z > 1$ are shown, which are considered to belong to clustered state.

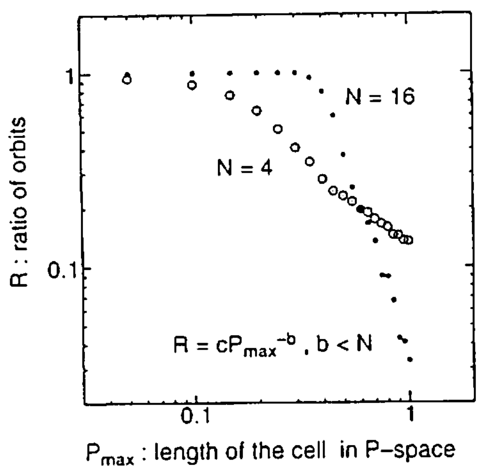

Figure 13. Relative volume of clustered states in the phase space, plotted as a function of hypercube cell length, for $N = 4$ and $N = 16$. $K = 0.3$. A total of 10^3 initial points are sampled to check if they are in a clustered state. The ratios of clustered orbits in an N-dimensional hypercube with the edge length P_{max} in the momentum space are plotted.

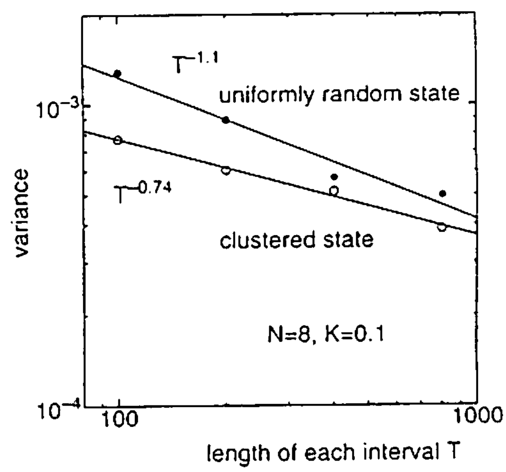

Figure 14. Variance of the short-time (maximal) Lyapunov exponents for a clustered state and the uniformly random state. In the clustered state the variance shows an anomalous power-law behaviour implying long time correlation, whereas the variance shows normal convergence to 0 in the uniformly random state. $N = 8$, $K = 0.1$.

The geometrical structure in phase space gives us a hint of a mechanism for the stabilization of the clustered state, as is shown in figures 11 and 12. Figure 11 shows a 2-dimensional slice of phase space for a 4-particle system. We measure the maximal Lyapunov exponent for a finite temporal interval t. If the initial condition (x_0, p_0) belongs to KAM tori the exponent $\lambda_{\max}(t)$ varies as $\lambda_{\max}(t) \propto 1/t$. In figures 11 and 12 dots indicate initial conditions where $\lambda_{\max}(t) < 1/\sqrt{t}$, which can be considered as belonging to KAM tori, islands, or their remnants. Clustered states are again estimated by the condition $Z > 1$ and are shown in figure 12. We note that they spread over the web structures of KAM tori and islands. The outer region has a complicated *fractal* structure as is shown in figure 13. In the figure, the relative volume of clustered states is plotted as a function of a length of the edge of the sampling cell $P_{\max}$. The volume $V(P_{\max})$ decays with a fractional power of the edge length $P_{\max}$ in the momentum space (e.g. $V(P_{\max}) \propto P_{\max}{}^{-3.2}$ for $N = 16$.) This result means that the outer region of clustered states has a fractal structure. For the central region, clustered states occupy almost all the volume, which seems to be supported by KAM tori and islands.

From the above observation, we reach the conjecture that the clustered state is strongly affected by the existence of remnants of KAM tori and islands. This conjecture is supported by examining the fluctuation properties of dynamical variables, e.g. Lyapunov exponents [29]. Suppose we measure a Lyapunov exponent for a finite interval, say T and denote it as $\lambda(T)$. Sampling $\lambda(T)$, we get a distribution of these short-time Lyapunov exponents. Here we study the T-dependence of the variance of this distribution. Since $\lambda(T)$ is calculated as a sum of stepwise expansion rates during T-steps as

$$\lambda(T) = \frac{1}{T} \sum_{t=1}^{T} \log\left(\frac{|\delta v(t)|}{|\delta v(t-1)|}\right) \tag{17}$$

we expect

$$(\Delta\lambda(T))^2 \propto \begin{cases} T^{-\alpha} & 0 < \alpha < 1 \quad \text{when long time correlation exists} \\ T^{-1} & \quad\quad\quad\quad\;\; \text{without long time correlation.} \end{cases} \tag{18}$$

Figure 14 clearly shows the existence of long time correlation in the clustered state but not in the random state. Thus the structure change from cluster to uniform chaos is understood as the transition from sticky motion to random motion without any spatiotemporal order.

6. Discussion

In this paper we have shown the existence of an ordering process (which we call a cluster) in *Hamiltonian* systems. This clustering is a remarkable novel feature in Hamiltonian systems distinguishable from uniform thermalization. The clustered states are chaotic and show crossover to uniform chaos, which is a chaos–chaos crossover. The theoretical study of the dynamical crossover between different chaotic seas for high-dimensional systems is an important area of future study, and is related to the recent study on the strong stochasticity threshold in high-dimensional Hamiltonian systems [27, 28].

Clustered states are long-lived and quasistationary especially in weak nonlinearity. The origin of stability of clustered states can be found in the intricate structure of a high-dimensional phase space. Indeed, torus-rich regions form a fractal structure in the phase space. For a regular orbit, this is the first discovery of such fractal structure, although it may be related to the fuzzy fat fractal for a stochastic layer [7].

The fluctuation of short-time Lyapunov exponents has revealed the sticky motion of a cluster. Preliminary data for the short-time diffusion coefficient [30] also support the existence of long-time correlation in a clustered state [31]. Lyapunov spectra and vectors have also demonstrated an internal mode for a clustered motion, clarifying order formation in a Hamiltonian system. Detailed Lyapunov analysis will be a powerful tool for exploring the high-dimensional phase space. An excellent application of Lyapunov analysis for a Hamiltonian map lattice is seen in [32]. Asymptotic behaviour of Lyapunov spectra for a system with a macroscopic state is also a subject for future study [17–20].

Ordered motion in high-dimensional chaos has been extensively investigated in dissipative systems. Clustering is an important notion in dissipative globally coupled maps [33]. Switching among ordered motions through high-dimensional chaos is found, and termed as *chaotic itinerancy* [33, 34]. Switching among our clustered motions and random chaos gives a clear example of chaotic itinerancy in Hamiltonian systems. We note that similar ordered motion is seen in molecular dynamics simulations for glass [35] and water [36]. Our clustered state may give a minimal basis for the theoretical understanding for the ordered motion in molecular dynamics.

Although the clustered state has a finite lifetime, the lifetime increases rapidly with the decrease of nonlinearity, suggesting some dependence analogous to Nekhoroshev's estimate. Thus, in a weakly nonlinear system, the clustered state is easily observed, and is stable over long time steps. This fact implies that our clustered state will be much more frequently seen in a Hamiltonian system with continuous time, since a proper limit with $K \to 0$ for our model gives a flow system of a time-independent Hamiltonian. Clustering processes will hopefully be found in other physical systems, such as gravitational systems, microclusters of atoms, nuclei, and so on. Chaos will give a new light on their study, in addition to traditional view based on barrier structures of potential energy landscapes.

Acknowledgments

We would like to thank Y Aizawa, K Ikeda, K Shinjo, T Yanagita, T Ikegami, T Kobayashi, Y Takahashi, I Ohmine, K Iwano and S Adachi for valuable discussions. TK thanks Professor K Nozaki and the members of R-Laboratory at Nagoya University for useful discussions. We are grateful to National Institute for Fusion Science at Nagoya for computational facility of FACOM VP200E, VP200 and M380. The present research is partially supported by Grant-in-Aids (Nos. 02302022, 03302018, 03740183 and 03740187) for Scientific Research from the Ministry of Education, Science, and Culture of Japan. We thank one of the referees for pointing out the sum rule for the inner product $s^{(k)}$. We also thank S Ishizaka for his excellent graphic software *'Ngraph'*.

References

[1] MacKay R S and Meiss J (ed) 1987 *Hamiltonian Dynamical Systems* (Bristol: Adam Hilger)
Lichtenberg A J and Lieberman M A 1983 *Regular and Stochastic Motion* (Berlin: Springer)
[2] Chirikov B V 1979 *Phys. Rep.* 52 263

[3] Sawada S 1987 *Microclusters* ed S Sugano *et al* (Berlin: Springer) p 211
[4] Konishi T and Kaneko K 1990 *J. Phys. A: Math. Gen.* **23** L715
[5] Kaneko K 1986 *Collapse of Tori and Genesis of Chaos in Dissipative Systems* (Singapore: World Scientific); 1989 Simulating Physics with Coupled Map Lattices *Formation, Dynamics, and Statistics of Patterns* ed K Kawasaki, A Onuki and M Suzuki (Singapore: World Scientific) pp 1–54, and references cited therein
[6] Froeschlé C 1972 *Astron. Astrophys.* **16** 172
[7] Kaneko K and Bagley R J 1985 *Phys. Lett.* **110A** 435
[8] Kook H-t and Meiss J 1989 *Physica* **35D** 65
[9] Kantz H and Grassberger P 1988 *J. Phys. A: Math. Gen.* **21** L127
[10] Kaneko K and Konishi T 1987 *J. Phys. Soc. Japan* **56** 2993
[11] Konishi T and Kaneko K 1989 *Cooperative Dynamics in Complex Physical Systems* ed H Takayama (Berlin: Springer) pp 320–2
[12] Konishi T 1989 *Prog. Theor. Phys. Suppl.* **98** 19
[13] Konishi T and Kaneko K, in preparation
[14] Benettin G, Galgani L, Giorgilli A and Strelcyn J M 1978 *C. R. Acad. Sci. Paris* A **286** 431
[15] Shimada I and Nagashima T 1979 *Prog. Theor. Phys.* **61** 1605
[16] Eckmann J-P and Ruelle D 1985 *Rev. Mod. Phys.* **57** 617
[17] Ruelle D 1982 *Commun. Math. Phys.* **87** 287
[18] Livi R *et al* 1986 *J. Phys. A: Math. Gen.* **19** 2033
[19] Newman C M 1986 *Commun. Math. Phys.* **103** 121
[20] Eckmann J-P and Wayne C E 1988 *J. Stat. Phys.* **50** 853; 1989 *Commun. Math. Phys.* **121** 147
[21] Kaneko K 1986 *Physica* **23D** 436
[22] Arnol'd V I 1964 *Sov. Math. Dokl.* **5** 581
[23] Holmes P J and Marsden J E 1983 *J. Math. Phys.* **23** 669
[24] Saito N *et al* 1969 *J. Phys. Soc. Japan* **27** 815
[25] Nekhoroshev N N 1977 *Russian Math. Surveys* **32** 1
[26] Lochak P 1990 *Phys. Lett.* **143A** 39
[27] Pettini M and Landolfi M 1990 *Phys. Rev.* A **41** 768
[28] Pettini M and Cerruti-Sola M 1991 *Phys. Rev.* A **44** 975
[29] Aizawa Y *et al* 1989 *Prog. Theor. Phys. Suppl.* **98** 36
[30] Kaneko K and Konishi T 1989 *Phys. Rev.* A **40** 6130
[31] Konishi T and Kaneko K, in preparation
[32] Falcioni M, Marini Bettolo Marconi U and Vulpiani A 1991 *Phys. Rev.* A **44** 2263
[33] Kaneko K 1989 *Phys. Rev. Lett.* **63** 219; 1990 *Physica* **41D** 38
[34] Ikeda K, Matsumoto K and Ohtsuka K 1989 *Prog. Theor. Phys. Suppl.* **99** 295
Tsuda I 1990 *Neurocomputers and Attention* ed A V Holden and V I Kryukov (Manchester: Manchester University Press)
[35] Shinjo K 1989 *Phys. Rev.* B **40** 9167; 1989 *J. Chem. Phys.* **90** 6627
[36] Ohmine I and Tanaka H 1990 *J. Chem. Phys.* **93** 8138, and references therein